Journal of Applied Polymer Science

A phosphorus-containing phenolic derivative and its application in benzoxazine resins: Curing behavior, thermal, and flammability properties

Siqi Huo, Jun Wang, Shuang Yang, Bin Zhang, Yushan Tang
Department of Materials Science and Engineering, Wuhan University of Technology, Wuhan 430070, People's Republic of China
Correspondence to: S. Yang (E-mail: 583377051@qq.com)

ABSTRACT: In this work, flame-retardant benzoxazine resins were prepared by copolymerization of bisphenol A based benzoxazine (BA-a) and a phosphorous-containing phenolic derivative (DOPO-HPM). The curing behavior, thermal stability, and flame resistance of BA-a/DOPO-HPM composites were studied by differential scanning calorimeter (DSC), thermogravimetric analysis (TGA), limited oxygen index (LOI) measurement, UL94 test, and cone calorimeter. The DSC results indicated that DOPO-HPM catalyzed the curing reaction because of its acidity. The TGA results revealed that the BA-a/DOPO-HPM thermosets possessed higher decomposition temperatures ($T_{5\%}$) and char yields than that of BA-a. The combustion tests indicated that the flame retardant properties of BA-a/DOPO-HPM thermosets were enhanced. The BA-a/DOPO-HPM-20 sample acquired the highest LOI value of 32.6% and UL94 V-0 rating. Moreover, the average of heat release rate (av-HRR), peak of heat release rate (pk-HRR), average of effective heat of combustion (av-EHC) and total heat release (THR) of BA-a/DOPO-HPM-20 were decreased by 24.6%, 53.1%, 14.9%, and 22.1%, respectively, compared with BA-a. The attractive performance of BA-a/DOPO-HPM blends was attributed to the molecular structure of DOPO-HPM composed of DOPO group with excellent flame-retardant effect and phenolic hydroxyl group with catalysis. © 2016 Wiley Periodicals, Inc. J. Appl. Polym. Sci. **2016**, *133*, 43403.

KEYWORDS: blends; flame retardance; thermal properties

Received 17 November 2015; accepted 31 December 2015
DOI: 10.1002/app.43403

INTRODUCTION

Benzoxazine resins, as a new class of thermosetting phenolic resins have been developed to overcome the shortcomings of traditional phenolic resins while keeping their advantages. Benzoxazine resins can be used as advanced matrix resins in microelectronics, aerospace and other industries due to their good thermal stability, flame retardancy, high glass transition temperature (T_g) with low water absorption and near zero shrinkage or expansion upon curing.[1–8] However, the polymer needs to be cured at relatively high temperature (180 °C or higher), which may lead to the degradation of polymer networks.[9–11] What's more, the flame resistance of benzoxazine resins constrain their application in high-performance materials. The development and application of high performance flame retardant benzoxazine resins have attracted extensive concern of researchers.

Traditionally, the flame retardancy of polymers can be improved by incorporating the halogenated compounds. Nevertheless, the applications of halogenated compounds are restricted due to environmental reasons.[12,13] Hence, nonhalogenated flame retardants have been widely applied in recent years. Among them, 9,10-dihydro-9-oxa-10-phosphaphenanthrene-10-oxide (DOPO) and its derivatives have attracted a great deal of attention due to their high reactivity, high thermal stability, and flame-retardant efficiency.[14–19] In the past decade, some literatures have reported the synthesis of DOPO-containing benzoxazine resins.[20–22] Compared with the complicated synthesis process, blending or copolymerizing with DOPO-based flame retardants may be a simple and efficient approach to enhance the flame retardancy of benzoxazine resins. However, few works about finding suitable DOPO-based flame retardants to enhance the flame retardancy of benzoxazine resins were reported.

In our previous report,[23] a phosphorous-containing phenolic flame-retardant (DOPO-HPM) was successfully prepared via the addition reaction between 9,10-dihydro-9-oxa-10-phosphaphenanthrene-10-oxide (DOPO) and *N*-(4-hydroxyphenyl) maleimide (HPM). It was found that the maleimide structure retarded the decomposition and improved the flame retardancy of resin matrix due to the rigid imide ring.[24–26] In addition, Agag and Takeichi[27,28] observed that introducing HPM into the benzoxazine resin initiated the ring-opening polymerization of

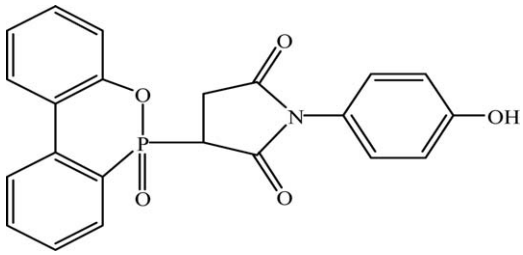

Figure 1. Chemical structure of DOPO-HPM.

the benzoxazine monomer and lowered the polymerization temperature of benzoxazine resin due to the acid character of HPM. Liu and Yu[29] also found that compared with *N*-Phenylmaleimide, HPM, and 4-maleimidobenzoicacid effectively promoted the polymerization of benzoxazine resin. Therefore, DOPO-HPM may be capable of enhancing the flame retardancy and decreasing the curing temperature of benzoxazine resins.

In this work, DOPO-HPM was employed to enhance the flame retardancy and lower the polymerization temperature of benzoxazine resins. The characteristic properties of the benzoxazine composites were investigated.

EXPERIMENTAL SECTION

Materials

BA-a type benzoxazine resin based on bisphenol-A, formaldehyde, and aniline was purchased from Haiso Technology. DOPO-HPM was synthesized in our group as per previous report,[23] and the structure of which is shown in Figure 1. Acetone was purchased from Sinopharm Chemical Reagent. All reagents were used without further purification.

Sample Preparation

BA-a and DOPO-HPM were dispersed in acetone under ultrasonic dispersing. The mixture was then evaporated at room temperature under vacuum. About 2.5 g of the mixture was fetched for DSC test and gelation experiment. The mixture was prepolymerized at 130 °C and then degassed under vacuum for 10 min. The mixture was poured into preheated mold and thermally cured in air convection oven at 160, 180, 200, and 220 °C for 2 h each. All the details of formula are listed in Table I.

Measurements

Differential scanning calorimetry (DSC) thermograms were recorded with Perkin–Elmer DSC 4000 at a heating rate of 10 °C/min under nitrogen atmosphere from 50 to 300 °C and an empty aluminum pan as a reference. The weights of the samples were 12 mg.

The LOI values were measured at room temperature on a JF-3 oxygen index meter (Jiangning Analysis Instrument Company, China) according to ISO 4589-2: 2006 standard and dimensions of all samples were 130 × 6.5 × 3 mm^3. Vertical burning (UL-94) tests were carried out on the NK8017A instrument (Nklsky Instrument, China) with the dimension of 130 × 13 × 3 mm^3 according to the UL-94 test standard. Cone calorimeter measurements were performed on an FTT cone calorimeter according to ISO 5660 standard under an external heat flux of 50 kW/m^2. The dimension of samples was 100 × 100 × 3 mm^3. The measurement for each specimen was repeated three times, and the error values of the typical cone calorimeter data were reproducible within ±5%.

Thermogravimetric analysis (TGA) was performed using NETZSCH STA449F3 at a heating rate of 10 °C/min under nitrogen atmosphere from 40 to 800 °C.

A knife flat method was used to test the gel time (t_{gel}) of resin. 2 g of a known weight of the resin simple was placed in the middle of the stainless steel plate which was heated to four different temperatures (T = 170 °C, 180 °C, 190 °C, 200 °C). In order to survey the trend of filamentation, the samples were picked up constantly by knife. The t_{gel} at each temperature was defined as from the beginning heating to that the samples could not form wire. And the activation energy (E_a) of the gelation process can be calculated from the gel times measured at different isothermal temperatures using the Arrhenius model. The relationship of t_{gel} and E_a is expressed as[30,31]:

$$\ln(t_{gel}) = \ln(A) + \left(\frac{E_a}{RT}\right)$$

where t_{gel} is the gel time (s), A is a pre-exponential factor, E_a is activation energy (kJ/mol), R is the ideal gas constant, and T is the temperature (K).

Fourier Transform Infrared (FTIR) spectra were obtained using a Nicolet 6700 infrared spectrometer. The powdered samples were thoroughly mixed with KBr and then pressed into pellets.

Morphological studies on the residual chars were conducted using a JSM-5610LV scanning electron microscope (SEM) at an acceleration voltage of 25 kV.

RESULTS AND DISCUSSION

Curing and Gelling Behaviors of Benzoxazine Resins

The curing behaviors of BA-a/DOPO-HPM resins were studied by DSC as shown in Figure 2. The DSC curve of BA-a resin was also taken for comparison. The detailed data were summarized in Table II. As can be seen in Table II, the exothermal initial temperature (T_i) for BA-a started at 192.3 °C, reached the maximum at 240.1 °C and the heat output (ΔH) was 200.5 J/g, which was the typical thermal curing characteristic of oxazine ring-opening polymerization. When adding 5 wt % contents of DOPO-HPM, the T_i and T_p appeared at 162.3 °C and 220.5 °C, respectively, approximately 30 °C and 19.6 °C, respectively, lower than that of BA-a. The ΔH of BA-a/DOPO-HPM-5 was 182.3 J/g, lower than that of BA-a. The ring-open polymerization of benzoxazine was an acidic-catalytic reaction.[28,32,33]

Table I. Formulas of the Cured Benzoxazine Resins

Sample code	BA-a (wt %)	DOPO-HPM (wt %)	*P* (wt %)
BA-a	100	0	0
BA-a/DOPO-HPM-5	95	5	0.38
BA-a/DOPO-HPM-10	90	10	0.77
BA-a/DOPO-HPM-15	85	15	1.15
BA-a/DOPO-HPM-20	80	20	1.53

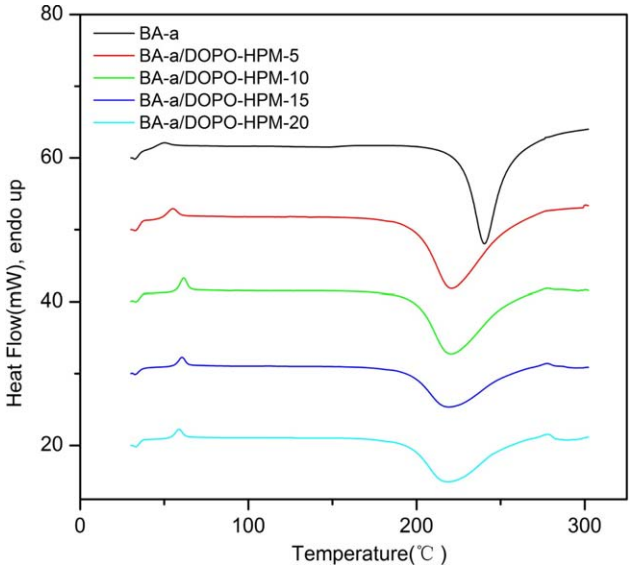

Figure 2. DSC thermograms of benzoxazine resins. [Color figure can be viewed in the online issue, which is available at wileyonlinelibrary.com.]

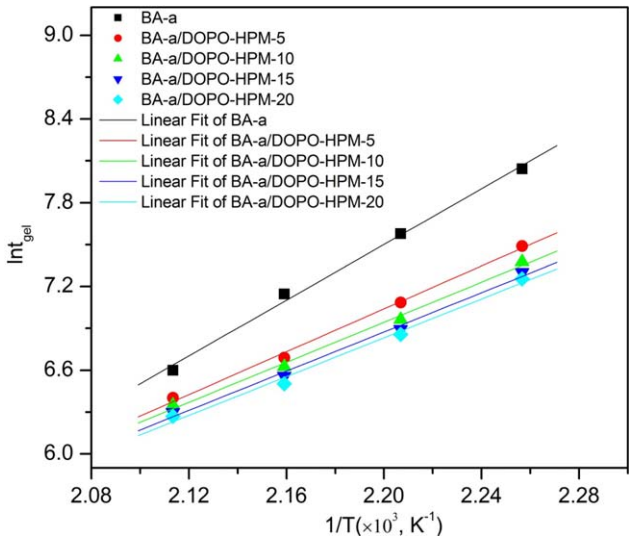

Figure 3. Arrhenius plots of benzoxazine resins. [Color figure can be viewed in the online issue, which is available at wileyonlinelibrary.com.]

Therefore, DOPO-HPM as an organic acid catalyst can effectively promote the ring opening reaction and lower the curing temperature. What's more, when further increasing the content of DOPO-HPM, the curing behaviors of BA-a/DOPO-HPM just changed a little, indicating that even a small amount of DOPO-HPM was enough for promoting the polymerization of BA-a.

The Arrhenius plots of benzoxazine resins were shown in Figure 3. The activation energies (E_a) estimated from the slopes of the lines was given in Table II. As shown in Table II, the E_a of BA-a was 83.0 kJ/mol, which was closed to the E_a (84 kJ/mol for benzoxazine) presented by Kasemsiri *et al.*[30] As with the ΔH trend, the E_a of BA-a resin decreased with the increasing DOPO-HPM content. This also indicated that DOPO-HPM had the ability to promote the ring-opening of BA-a and accelerate the process.

Thermal Properties of the Cured Benzoxazine Resins

The glass transition temperatures (T_gs) of the cured BA-a and BA-a/DOPO-HPM resins were measured by DSC and the results were summarized in Table III. The T_g value of the cured BA-a/DOPO-HPM resins (163.6 − 167.4 °C) and the cured BA-a resin (168.3 °C) were basically consistent. DOPO-HPM with bulky rigid group increased the rotational barrier of the thermosets which may be the reason of keeping the stability of T_g Value.

Thermal properties of DOPO-HPM and the cured benzoxazine resins were measured by TGA in nitrogen atmosphere. The TGA and DTG curves were shown in Figure 4. The characteristic thermal decomposition data, such as temperature at 5% weight loss ($T_{5\%}$), temperature at maximum weight loss rate (T_{max}) and char yields at 800 °C were listed in Table III. As shown in Figure 4, DOPO-HPM showed good stability over 300 °C and had a strong DTG peak at 410.3 °C (T_{max1}). The char yield of DOPO-HPM at 800 °C is 28.5%, exhibiting a certain charring performance.

As shown in Figure 4, the cured BA-a resin presented three stages of weight loss. The first weight loss stage was attributed to the evaporation of various amines from the Mannich bridge cleavage, the second one was related to the breakup of isopropylidene linkage of Bisphenol-A backbone, and the third one was assigned to the release of substituted benzene compounds from the degradation of the char which overlapped with the second stage (centered near 460 °C).[9,34,35] In the first weight loss stage, it was obvious that when adding DOPO-HPM, the DTG peak area decreased and the $T_{5\%}$ of the cured BA-a/DOPO-HPM resins increased, which was possibly owing to the fact that DOPO-HPM had good thermal stability and retarded the decomposition of BA-a before 300 °C. In the main decomposition stage,

Table II. Thermal Cure Characteristics of Benzoxazine Resins

Simple code	T_i (°C)[a]	T_p (°C)[b]	T_e (°C)[c]	ΔH (J/g)	E_a (kJ/mol)
BA-a	192.3	240.1	268.3	200.5	83.0
BA-a/DOPO-HPM-5	162.3	220.5	266.2	182.3	63.9
BA-a/DOPO-HPM-10	157.8	219.4	267.3	168.1	59.7
BA-a/DOPO-HPM-15	155.4	218.6	266.8	126.8	58.4
BA-a/DOPO-HPM-20	155.1	218.3	265.6	120.3	57.8

[a] T_i indicates the exothermal initial temperature.
[b] T_p indicates the exothermal peak temperature.
[c] T_e indicates the exothermal end temperature.

Table III. Thermal Properties of the Cured Benzoxazine Resins

Simple code	T_g (°C)	$T_{5\%}$ (°C)	T_{max1} (°C)	T_{max2} (°C)	T_{max3} (°C)	Char yields at 800 °C (%)	
						Experimental value	Calculated value
DOPO-HPM	—	348.3	410.3	—	—	28.5	—
BA-a	168.3	252.9	197.1	384.1	—	31.4	—
BA-a/DOPO-HPM-5	163.6	280.1	189.1	345.1	408.2	33.6	31.3
BA-a/DOPO-HPM-10	167.1	285.8	189.8	343.8	425.6	35.1	31.1
BA-a/DOPO-HPM-15	167.2	278.6	192.9	336.9	426.3	36.4	30.9
BA-a/DOPO-HPM-20	167.4	278.2	190.2	332.2	417.1	37.4	30.8

the T_{max2} of the cured BA-a/DOPO-HPM resins decreased and the T_{max3} appeared with the addition of DOPO-HPM. It was deduced that the pyrolysis of DOPO groups over 300 °C accelerated the degradation of Bisphenol-A backbone, which resulted in the decrease of T_{max2} and the appearance of T_{max3}. The char yields of the cured BA-a/DOPO-HPM resins were higher than that of BA-a from 400 to 800 °C as shown in Figure 4, and the experimental values of char yields of the cured BA-a/DOPO-HPM were higher than the calculated ones at 800 °C as listed in Table III, suggesting that the incorporation of DOPO-HPM obviously increased the char yield of resin matrix.

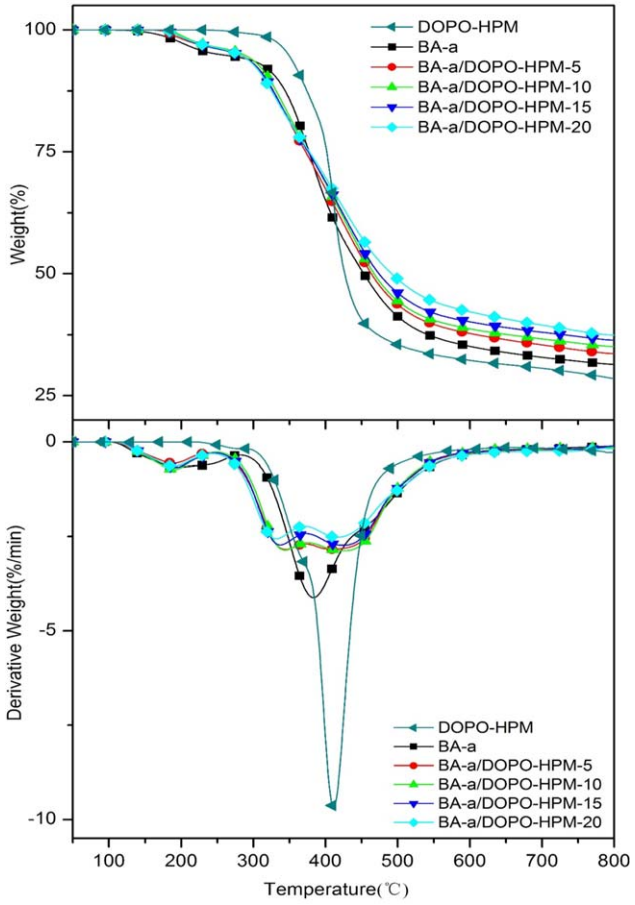

Figure 4. TG and DTG curves of DOPO-HPM and the cured benzoxazine resins under N_2 atmosphere. [Color figure can be viewed in the online issue, which is available at wileyonlinelibrary.com.]

LOI and UL94 Rating Tests

The flame retardancy of the cured BA-a and BA-a/DOPO-HPM composites were initially measured by LOI and UL94 vertical burning tests. The relevant data were shown in Table IV. As can be seen, the LOI of the cured BA-a resin was 24.8%, whereas the presence of phosphorus increased the LOI even when the phosphorus content was low. The LOI was increased with the increasing content of phosphorus and finally reached 32.6% with 1.53 wt % of phosphorus content. Meanwhile, the classification of V-0 rating was achieved with only 0.77 wt % of phosphorus content. The higher LOI values and UL94 rating with relatively lower amount of phosphorus confirmed that DOPO-HPM can improve the flame retardant properties of the BA-a resin. As discussed in TGA, the char yields also increased with the increasing DOPO-HPM content. Higher char yield was able to reduce the release of pyrolysis gas and heat during combustion, consequently to improve the flame resistance of benzoxazine resins.

Cone Calorimeter Analysis of the Cured Benzoxazine Resins

The cone calorimetry test is one of the most effective methods for evaluating the flammability of materials. The characteristic parameters, including average of heat release rate (av-HRR), peak of heat release rate (pk-HRR), average of effective heat of combustion (av-EHC), total heat release (THR), average CO yield (av-COY), average CO_2 yield (av-CO_2Y), and char yields at 500 s are listed in Table V.

The heat release rate (HRR) curves of the cured BA-a and BA-a/DOPO-HPM resins are shown in Figure 5. As shown in Figure 5, the cured BA-a resin burned rapidly after ignition and

Table IV. LOI and UL94 Test Results of the Cured Benzoxazine Resins

Sample code	*P* (wt %)	LOI (%)	UL-94 grade
BA-a	0	24.8	V-1
BA-a/DOPO-HPM-5	0.38	27.1	V-1
BA-a/DOPO-HPM-10	0.77	29.2	V-0
BA-a/DOPO-HPM-15	1.15	31.5	V-0
BA-a/DOPO-HPM-20	1.53	32.6	V-0

Table V. Cone Results of the Cured Benzoxazine Resins

Sample code	av-HRR (kW/m^2)	pk-HRR (kW/m^2)	av-EHC (MJ/kg)	THR (MJ/m^2)	av-COY (kg/kg)	av-CO_2Y (kg/kg)	Char yields at 500 s (%)
BA-a	171	751	25.4	77.5	0.088	1.563	19.8
BA-a/DOPO-HPM-5	136	469	23.1	66.7	0.118	1.296	25.5
BA-a/DOPO-HPM-10	136	467	22.7	63.9	0.124	1.275	27.5
BA-a/DOPO-HPM-15	134	446	22.3	62.5	0.133	1.247	28.7
BA-a/DOPO-HPM-20	129	352	21.6	60.4	0.143	1.206	30.1

only one sharp HRR peak appeared with the peak value of 751 kW/m^2. In addition, the cured BA-a resin had the highest av-HRR of 171 kW/m^2. In contrast, the pk-HRR and av-HRR of the cured BA-a/DOPO-HPM resins reduced strongly. For example, the pk-HRR and av-HRR of the cured BA-a/DOPO-HPM-20 resin decreased by 53.1% and 24.6%, respectively. This phenomenon suggests that DOPO-HPM effectively reduced the HRR. Further confirmation is provided for the total heat release (THR) as given in Table V.

Av-EHC, which is the ratio of average of heat release rate (av-HRR) to the average mass loss rate from the cone calorimetry test, discloses the burning degree of volatile gases in gas-phase flame. As presented in Table V, the av-EHC of the cured BA-a resin was the highest in all samples. The av-EHC value gradually decreased with the increasing mass fraction of DOPO-HPM. The results indicated that the flame-retardant effect of DOPO-HPM was partly exerted in the gaseous-phase through flame-retardant quenching effect. This was further confirmed by av-COY and av-CO_2Y. As shown in Table V, the av-COY of the cured BA-a/DOPO-HPM resins increased, whereas the av-CO_2Y decreased with the increase of DOPO-HPM contents compared with those of the cured BA-a resin. It showed that the gaseous-phase pyrolysis products of DOPO-HPM with quenching effect restrained the ignition of combustible volatiles, thus resulting in more incomplete combustion products (CO) and less complete combustion products (CO_2).[36]

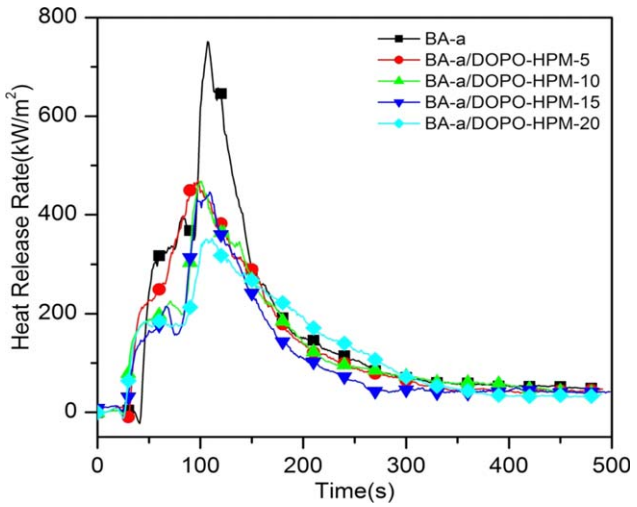

Figure 5. HRR curves of the cured benzoxazine resins. [Color figure can be viewed in the online issue, which is available at wileyonlinelibrary.com.]

As shown in Table V, the cured BA-a had the lowest residual weight of 19.8% among all the samples. With the increasing content of DOPO-HPM, the residual weight of the cured BA-a/DOPO-HPM resins increased, demonstrating that DOPO-HPM also functioned in the condensed-phase and availably improved the char yield, which was in agreement with the TGA results discussed above.

Based on the above discussion, it can be deduced that DOPO-HPM simultaneously worked in the gaseous-phase and condensed-phase, imparting good flame-retardant performance to the BA-a/DOPO-HPM composites.

FTIR Study of the Residual Chars after UL94 Tests

Figure 6 showed the FTIR spectra of the residual chars of the cured BA-a and BA-a/DOPO-HPM resins after UL94 test. The absorption peak at 1596 cm^{-1} assigning to the phenyl structure can be observed in all spectra curves. It was worth noting that the absorption peak at 1596 cm^{-1} became more and more obvious with the addition of DOPO-HPM. For the BA-a/DOPO-HPM thermosets, apart from the absorption peak at 1596 cm^{-1}, new absorption peaks at 1710, 1376, 1196, 1116, and 916 cm^{-1} appeared. The obvious absorption peaks of C═O at 1710 cm^{-1} and C—N at 1376 cm^{-1} indicated the residual fragments of maleimide group, suggesting that the maleimide groups were carbonized and retarded the decomposition of the BA-a thermosets during combustion. In addition, the new absorbance peaks of P—O—Ph at 1196, 1116, and 916 cm^{-1}

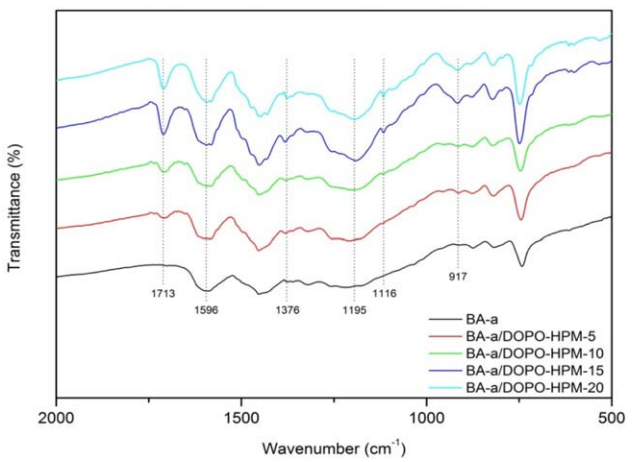

Figure 6. FTIR spectra of the residual chars after UL94 test. [Color figure can be viewed in the online issue, which is available at wileyonlinelibrary.com.]

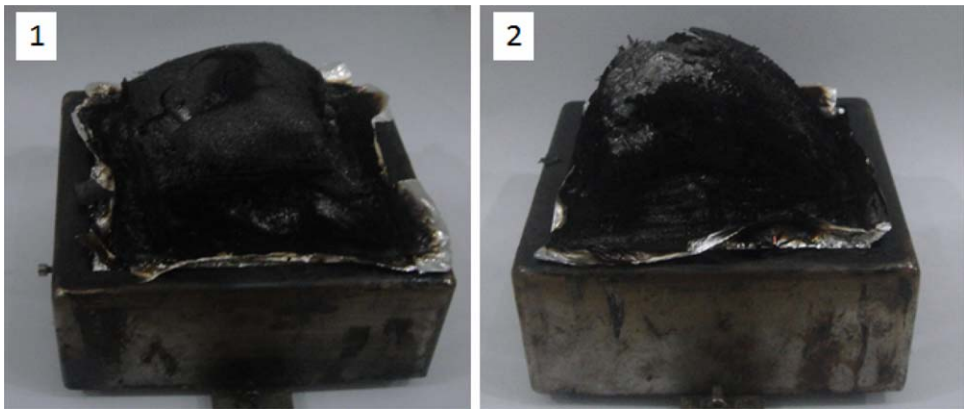

Figure 7. Digital images of the residual chars after cone calorimeter test: (1) BA-a; (2) BA-a/DOPO-HPM-20. [Color figure can be viewed in the online issue, which is available at wileyonlinelibrary.com.]

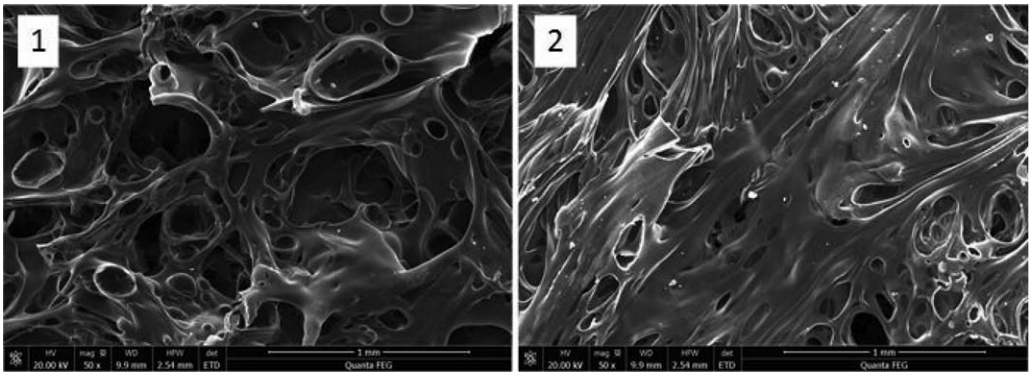

Figure 8. SEM images of the residual chars after the cone calorimeter test: (1) BA-a; (2) BA-a/DOPO-HPM-20.

further proved that DOPO group promoted the formation of phosphorus-rich char, which served as protective char layers for the underlying matrix.

Morphology and Element Composition of the Residual Chars after Cone Calorimeter Test

Figure 7 showed the digital images of the residual chars after cone calorimeter test. As shown in Figure 7, both of the BA-a and BA-a/DOPO-HPM-20 composite can form intumescent char layer after cone calorimeter test. However, the residual char yield and expansion ratio of the BA-a/DOPO-HPM-20 composite were higher than those of BA-a.

The residual chars were further investigated by scanning electron microscope (SEM) as shown in Figure 8. The char layer of the cured BA-a resin exhibited a multihole structure which was unable to serve as a protective layer after cone calorimeter test. However, the BA-a/DOPO-HPM-20 composite had a more continuous and compact surface of the char residue. The continuous and compact surface of the char residue prevented the release of pyrolysis gases and reduced the efficiency of heat- and oxygen-exchange. The intumescent char layer with a more continuous and compact surface effectively improved the flame retardancy.

Additionally, the element contents of the residual chars after cone calorimeter test were measured by EDS. The results were reported in Table VI. The phosphorus contents of the residual chars increased with the increasing content of DOPO-HPM. The phosphorus content was up to 1.12 wt % in the residual char of the BA-a/DOPO-HPM-20 composite. The result indicated that part of the DOPO groups decomposed to form phosphate and polyphosphate in condensed phase which promoted the charring of BA-a matrix to form phosphorus-rich viscous char layer during combustion.[25,37] The same trend was also observed in the oxygen contents of the residual chars, indicating the formation of high oxidation-resistance char layers.

CONCLUSIONS

In this work, DOPO-HPM was applied to modify BA-a. DOPO-HPM not only reduced the curing temperature, but also improved the flame retardancy of BA-a. DOPO-HPM accelerated the ring-opening polymerization of BA-a because of its acid character. TGA results revealed that BA-a/DOPO-HPM

Table VI. EDS Data of the Residual Chars after the Cone Calorimeter

	Element content (wt %)			
Sample code	C	N	O	P
BA-a	80.15	9.80	10.05	—
BA-a/DOPO-HPM-10	78.80	9.15	11.56	0.49
BA-a/DOPO-HPM-20	76.16	9.28	13.44	1.12

thermosets possessed higher char yields than that of BA-a. Combustion tests showed that the flame retardancy of BA-a/DOPO-HPM composites was promoted with the incorporation of DOPO-HPM. Therefore, the BA-a/DOPO-HPM composites with good processibility and flame retardancy can be used as the matrix resin of advanced composite materials.

REFERENCES

1. Ishida, H.; Allen, D. J. *Polymer (Guildf).* **1996**, *37*, 4487.
2. Huang, J.; Yang, S. *Polymer* **2005**, *46*, 8068.
3. Sawaryn, C.; Landfester, K.; Taden, A. *Macromolecules* **2010**, *43*, 8933.
4. Xu, M.; Yang, X.; Zhao, R.; Liu, X. *J. Appl. Polym. Sci.* **2013**, *128*, 1176.
5. Xu, Hu, M.; Zou, J.; Liu, X.; Dong, M.; Zou, S.; Liu, Y. X. *J. Appl. Polym. Sci.* **2013**, *129*, 2629.
6. Yan, H.; Jia, X. Y.; Li, M. L.; Li, T. T. *J. Appl. Polym. Sci.* **2013**, *129*, 3150.
7. Wang, D.; Li, B.; Zhang, Y.; Lu, Z. *J. Appl. Polym. Sci.* **2013**, *127*, 516.
8. Rimdusit, S.; Tiptipakorn, S.; Jubsilp, C.; Takeichi, T. *React. Funct. Polym.* **2013**, *73*, 369.
9. Yee Low, Ishida, H. H. *Polymer (Guildf).* **1999**, *40*, 4365.
10. Ishida, H.; Sanders, D. P. *Polymer (Guildf).* **2001**, *42*, 3115.
11. Low, H. Y. E. E.; Ishida, H. *Polym. Sci. Part B: Polym. Phys.* **1998**, *0488*, 1935.
12. Liang, B.; Cao, J.; Hong, X.; Wang, C. *J. Appl. Polym. Sci.* **2013**, *128*, 2759.
13. Zang, Wagner, L.; Ciesielski, S.; Müller, M.; Döring, P. M. *Polym. Adv. Technol.* **2011**, *22*, 1182.
14. Perret, Schartel, B.; Stöß, B.; Ciesielski, K.; Diederichs, M.; Döring, J.; Krämer, M.; Altstädt, J. V. *Eur. Polym. J.* **2011**, *47*, 1081.
15. Schartel, B.; Balabanovich, A.; Braun, I.; Knoll, U.; Artner, U.; Ciesielski, J.; Döring, M.; Perez, M. R.; Sandler, J. K.; Altstädt, W.; Hoffmann, V.; Pospiech, T. D. *J. Appl. Polym. Sci.* **2007**, *104*, 2260.
16. Schäfer, A.; Seibold, S.; Lohstroh, W.; Walter, O.; Döring, M. *J. Appl. Polym. Sci.* **2007**, *105*, 685.
17. Qian, L. *Polymer (Guildf).* **2011**, *52*, 5486.
18. Perret, B.; Schartel, B.; Stöß, K.; Ciesielski, M.; Diederichs, J.; Döring, M.; Krämer, J.; Altstädt, V. *Macromol. Mater. Eng.* **2011**, *296*, 14.
19. Xiong, Y.; Zhang, X.; Liu, J.; Li, M.; Guo, F.; Xia, X.; Xu, W. *J. Appl. Polym. Sci.* **2012**, *125*, 1219.
20. Su, H.; Liu, Z. *J. Therm. Anal. Calorim.* **2013**, *114*, 1207.
21. Spontón, Lligadas, M. G.; Ronda, J.; Galià, C.; Cádiz, M. V. *Polym. Degrad. Stab.* **2009**, *94*, 1693.
22. Lin, C. H.; Lin, H. T.; Chang, S. L.; Hwang, H. J.; Hu, Y. M.; Taso, Y. R.; Su, W. C. *Polymer (Guildf).* **2009**, *50*, 2264.
23. Yang, S.; Wang, J.; Huo, S.; Cheng, L.; Wang, M. *Polym. Degrad. Stab.* **2015**, *119*, 251.
24. Yang, S.; Wang, J.; Huo, S.; Cheng, L.; Wang, M. *Polym. Degrad. Stab.* **2015**, *115*, 63.
25. Yang, Wang, S.; Huo, J.; Wang, S.; Cheng, M. L. *Ind. Eng. Chem. Res.* **2015**, *54*, 7777.
26. Chen, X.; Gu, A.; Liang, G.; Yuan, L.; Zhuo, D.; Hu, J. *Polym. Degrad. Stab.* **2012**, *97*, 698.
27. Takeichi, Agag, T.; Zeidam, T. R. *J. Polym. Sci. Part A: Polym. Chem.* **2001**, *39*, 2633.
28. Agag, T.; Takeichi, T. *High Perform. Polym.* **2001**, *13*, S327.
29. Liu, Y. L.; Yu, J. M. *J. Polym. Sci. Part A: Polym. Chem.* **2006**, *44*, 1890.
30. Kasemsiri, S. R. P.; Hiziroglu, S. *Thermochim. Acta* **2011**, *520*, 84.
31. Gough, L. J.; Smith, I. T. *J. Appl. Polym. Sci.* **1960**, *3*, 362.
32. Dunkers, J.; Ishida, H. *J. Polym. Sci. Part A: Polym. Chem.* **1999**, *37*, 1913.
33. Agag, Tsuchiya, T.; Takeichi, H. T. *Polymer (Guildf).* **2004**, *45*, 7903.
34. Ishida, H.; Sanders, D. P. *Macromolecules* **2000**, *33*, 8149.
35. Ishida, H.; Sanders, D. P. *J. Polym. Sci. Part B: Polym. Phys.* **2000**, *38*, 3289.
36. Qian, L.; Qiu, Y.; Sun, N.; Xu, M.; Xu, G.; Xin, F.; Chen, Y. *Polym. Degrad. Stab.* **2014**, *107*, 98.
37. Xu, M. J.; Xu, G. R.; Leng, Y.; Li, B. *Polym. Degrad. Stab.* **2016**, *123*, 105.